Toward Safe and Smart Mobility: Energy-Aware Deep Learning for Driving Behavior Analysis and Prediction of Connected Vehicles

Yang Xing, *Member IEEE*, Chen Lv, *Senior Member, IEEE*, Xiaoyu Mo, Zhongxu Hu, Chao Huang, Peng Hang

***Abstract*—Connected automated driving technologies have shown tremendous improvement in recent years. However, it is still not clear how driving behaviors and energy consumption correlate with each other and to what extent these factors related to connected vehicles can influence the motion prediction performance. The precise recognition of driving behaviors and prediction of the vehicle motion is critical to the driving safety for connected automated vehicles (CAVs). Hence, in this study, an energy-aware driving pattern analysis and motion prediction system are proposed for CAVs using a deep learning-based time-series modeling approach. First, energy-aware longitudinal acceleration and deceleration behaviors and lateral lane-change behaviors are statistically analyzed. Then, a sliding standard deviation (SSD) test is applied to evaluate the smoothness of the trajectory and velocity signals considering different energy consumption levels. An energy-aware personalized joint time-series modeling (PJTSM) approach based on a deep recurrent neural network (RNN) and long short-term memory (LSTM) cell are proposed for accurate motion (trajectory and velocity) prediction of the leading vehicle. Finally, the differences in the prediction performance regarding different energy consumption levels are compared and discussed. It is shown that due to the higher randomness of the driving behaviors, the prediction accuracy for heavy energy users is the lowest among the three categories, which means it is harder to anticipate the driving behaviors of cars exhibiting heavy energy consumption. The personalized estimation of driving behaviors of CAVs will contribute to safer automated driving and transportation systems.**

***Index Terms*— Energy-aware driving behaviors, vehicle state prediction, time-series modeling, deep learning.**

I. Introduction

A. Motivation

Connected automated driving vehicles (CAVs) are gaining increasing attention from both areas of academia and industry. Vehicular technologies and automation are believed to be two of the cornerstones of next-generation automated driving vehicles [1,2]. Vehicular technologies and connected vehicles enable the understanding and prediction of driving intents as well as the driving styles of surrounding vehicles [3,4]. Moreover, vehicle energy consumption can be significantly reduced by connected and cooperative autonomous vehicles through moderate driving and platooning techniques [5,6]. Energy consumption, driving behaviors, and motion prediction are three key aspects that can dynamically interact with each other to form the motion behavior of connected vehicles [7,8]. It is known that different driving behaviors and driving styles can cause different levels of energy consumption [9,10]. For instance, in [11], it was stated that the energy consumption of the vehicle could be determined by three key factors, which are driver, vehicle, and traffic context. Among these, driving behaviors and styles can influence energy consumption most significantly. Existing studies mainly focus on the study of how driving behaviors can influence vehicle energy consumption. While, how energy-aware driving behaviors influence the accuracy of the predicted vehicle motion, and how energy consumption can be connected with other driving behavior related techniques, such as the trajectory prediction still need to be exploited before CAVs can fully realize their potential in the optimization of future transportation systems.

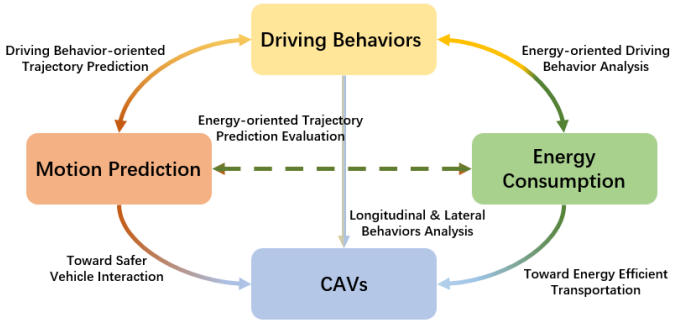

Fig. 1. Illustration of the analytical protocol for the relationships among energy consumption, driving behaviors, and motion prediction for connected vehicles.

Considering these aspects, in this study, an energy-aware vehicle motion (i.e., the trajectory and velocity) prediction model based on a deep learning method is proposed. An illustration of the research protocol is shown in Fig. 1. First, the longitudinal and lateral behaviors of the leading vehicle regarding different energy consumption levels are statistically analyzed to exploit the relationship between energy consumption and the corresponding driving behaviors. Then, a personalized joint time-series modeling network considering

Y. Xing, C. Lv, XY. Mo, C. Huang, ZX. Hu, P. Hang are with the School of Mechanical and Aerospace Engineering, Nanyang Technological University, 639798, Singapore. (e-mail: mailto:xing.yang, lyuchen, xiaoyu006, zhongxu.hu, chao.huang, hang.peng@ntu.edu.sg)..

the energy consumption level is proposed for the precise prediction of future vehicle states. Last, the comparison of the prediction results regarding different energy consumption levels and driving behaviors will be made to build the connections and analysis of the relationship between energy consumption and vehicle motion prediction. In sum, the holistic analysis of driving behaviors, energy consumption, and the prediction of the state will contribute to safer interaction strategies and energy-efficient transportation systems for the future design of CAVs.

B. Literature Review

Studies on driving behaviors and vehicle energy consumption, emissions, and battery optimization have been widely studied in the past two decades. The relationship between the energy management strategy (EMS) and the driving behavior-oriented micro-trip intensity for the electric vehicles was studied in [12]. It was shown that the high-intensity micro-trips influence the EMS more significantly than the low-intensity micro-trips. In [13], three driving styles, namely, aggressive, mild, and gentle, were defined based on the average acceleration. The driving styles were proved to have a considerable effect on energy consumption and can be affected by traffic flow. In [14], the authors developed an unsupervised learning-based parallel spectral clustering algorithm for driving behavior recognition. It was found that drivers who change the speed moderately and drive and relatively low speed lead to low fuel consumption. Similarly, in [15], a mobile platform for driving styles and fuel consumption was developed. The aggressive driving style can cause heavy energy consumption with fast start and acceleration, sudden speed change, and driving at high engine revolutions. In [16], it was found that the aggressive driving style, heavy braking, and less use of regenerative braking can cause more energy consumption and emission to the electric vehicle.

As shown in existing studies, the relationship between the driving behaviors and energy consumption can be mainly studied from two aspects, which are driving style-oriented energy consumption classification and energy management strategy optimization by integrating the driving behaviors and driving cycles [17,18]. The conventional approach mainly focuses on the analysis of the energy consumption of the whole trip, which can provide a macro-scope analysis for the driving behavior and energy usage [19]. While the micro-scope and real-time analysis for the energy consumption and driving behaviors are also important as it can contribute to a dynamic energy-aware driving behavior recognition system. Moreover, such a system can be further integrated into the vehicle states (such as trajectory and velocity) prediction system to improve driving safety.

The prediction of the motion of surrounding vehicles is another important task of future automated driving vehicles, as the vehicle has to make a proper decision, plan a future path, and generate courtesy interactions with neighboring entities [20]. It is shown that different driving styles and driving behaviors can also influence the vehicle state prediction accuracy [21]. Precise motion prediction of other vehicles requires a comprehensive analysis of vehicle states and driving behaviors. Moreover, realizing more driving patterns of the other entities will enhance the situation awareness of the intelligent vehicle and contribute to holistic intelligence in traffic context description, decision-making, and efficient planning [22]. Motion prediction, such as trajectory and velocity prediction, enables intelligent vehicles to have a strong capability of anticipating the intended maneuvers of surrounding vehicles and foreseeing dangerous and complicated situations, such as insoluble ethical issues [23]. Studies on vehicle motion prediction have been well-reviewed in [24], where three types of methods, namely, physics-based motion models [25,26], maneuver-based models [27,28], and interaction-aware motion models [29-30], are presented. Among these, the interaction-aware model can capture the interacting behaviors of the surrounding vehicles and generate a more precise estimation of future motion.

Most of the current studies on vehicle trajectory prediction focus on the construction of an interaction-aware model with machine learning and deep learning techniques [31-34], such as the Bayesian approach and deep sequential neural networks. For instant, in [35], a Bayesian approach for personalized driver model and model-based vehicle trajectory prediction system was developed. In [36], an interaction-aware intention and maneuver prediction framework were proposed. A game-theoretic algorithm was applied to estimate the intentions of surrounding entities iteratively. Then, a Bayesian network was implemented to predict future maneuvers and enhance the algorithm robustness for the unseen scenarios. In [37], an integrated Bayesian approach for maneuver-based trajectory prediction was developed. The system can efficiently process the driving maneuver and motion uncertainty of the surrounding vehicles with an arbitrary static environment.

The deep learning approach requires large-scale data for model training and evaluation. However, the advantages of the prediction accuracy and robustness are also significant dues to the strong ability in the learning of long-term dependence between interacting vehicles [38-40]. For example, in [41], an intention-aware trajectory prediction system was developed to automatically learn the spatial-temporal features based on a dual LSTM model. In [42], an ensemble RNN model was developed to predict the path of the obstacle vehicle. The previous two seconds of motion signals from Lidar, camera, or GPS are fused, and the next two-second trajectory is predicted using the ensemble RNN model. Similarly, in [43], an LSTM-based trajectory prediction model was proposed considering different driving styles for connected vehicles. In [44], a long-term interactive trajectory prediction model for surrounding vehicles trajectory prediction was proposed based on a hierarchical multi-sequence learning network. The high-level dependencies among the interacting vehicles can be captured with the proposed structural-LSTM network. Besides the LSTM-based networks, the generative adversarial model training-enabled networks can also be implemented in the trajectory prediction system. For instance, in [45], a generative adversarial imitation learning (GAIL) method was developed based on the Next Generation Simulation (NGSIM) dataset. The GAIL network can learn emergent driving behaviors using reinforcement learning and generate a high likelihood of expert

actions. Similarly, a social-bicycle generative adversarial network was proposed for trajectory prediction with multiple-interacting agents [46]. A graph attention network was used to encode the social interaction behaviors, and a recurrent encoder-decoder network was trained adversarial to predict future trajectories.

Although a series of achievements have been attained recently in motion prediction for connected vehicles, there is still a lack of in-depth analysis of the factors that can determine the performance of motion prediction and the impact of different driving behaviors on vehicle motion prediction. Moreover, few studies have connected energy consumption and motion prediction together to gain a comprehensive understanding of the traffic context. To the best of our knowledge, this is the first study that jointly considers energy consumption, driving behaviors, and motion prediction with a holistic framework and exploits the different prediction results considering energy consumption and driving behaviors.

C. Contribution

The contribution of this study can be summarized as follows.

1) First, the energy-aware longitudinal and lateral driving behaviors are studied and statistically analyzed with naturalistic data. Then, the smoothness of motion behavior (trajectory and velocity) regarding different energy usage levels are evaluated to study the energy-aware driving behaviors further. The energy-aware driving behavior analysis can contribute to efficient management for the CAVs-enabled transportation system.
2) Second, an energy-aware PJTSM system is proposed for vehicle motion prediction. The future trajectory and the velocity states of the leading vehicle can be precisely predicted. The system is important to an interaction-aware motion prediction system for the CAVs toward safer and efficient interaction.
3) Last, based on the motion prediction results, comparisons are made among the different energy consumption levels. It is found that the motion of heavy energy users is more difficult to predict and will generate more significant prediction errors than for light energy users, which shows the necessity of designing personalized motion predictors for future CAVs.

D. Paper Organization

The remainder of this paper is organized as follows. Section II introduces the high-level framework and research protocol of this study. In Section III, the energy-aware driving pattern and motion behavior are analyzed. In Section IV, the model construction process is described. The experimental results and model evaluation of the motion prediction and interclass performance comparison are represented in Section V. In Section VI, a discussion on the proposed model, along with future works, is given. Finally, the study is concluded in Section VII.

II. System Overview

In this section, the high-level framework of the proposed study and the description of each module are introduced. Five key modules in this study are established, namely, naturalistic data processing, energy consumption classification, energy-aware driving behavior analysis and assessment, motion prediction, and performance comparison modules. The connections and research methods are described as follows.

In this study, the NGSIM dataset is used for naturalistic highway driving behavior analysis and prediction. Specifically, the US Highway 101 dataset and Interstate 80 Freeway dataset are studied. Each vehicle has a unique identity and different frames. The sampling rate is 10 Hz. The NGSIM contains three types of vehicles: cars, motors, and trucks. Among these vehicles, cars are the majority type and will be used in the following analysis. As discussed in [47], NGSIM data can be noisy, and sometimes significant data errors exist. For example, in some cases, the vehicle can generate a collision path, which is abnormal in the real world [48]. Therefore, in this study, data preprocessing is applied to clean the raw dataset before further analysis. The data cleaning procedure given in [48] was partially adopted. The data processing part contains two steps:

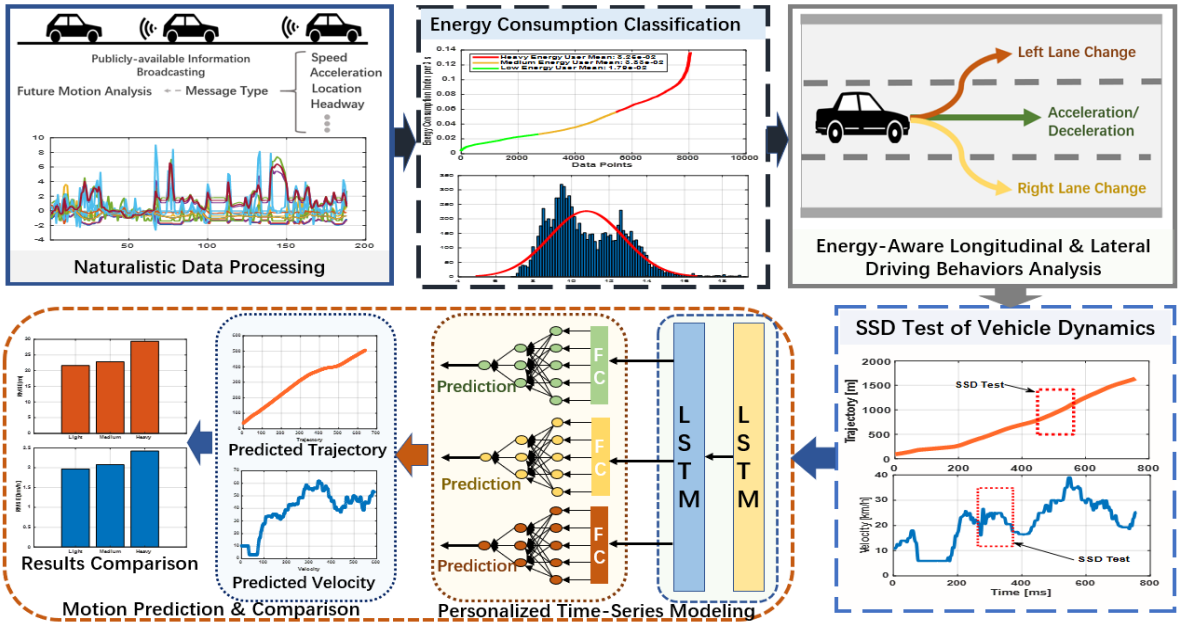

Fig. 2. High-level system architecture.

outlier removal and smoothing. The outlier removal module will detect significant error points and impossible kinematics such as sudden changes to a speed of zero, impossibly high acceleration values, or sudden headway spaces of zero. Significantly abnormal points, which are ten times larger than the mean value, will be regarded as unusual cases and will be replaced with a value based on interpolation of the nearby data. Then, the data will be filtered with a low-pass filter with a 10-Hz sampling rate and a 1-Hz passband.

The energy consumption classification module will first calculate the energy consumption every three seconds for each vehicle. The reason for selecting a duration of three seconds is that it is usually long enough to finish a driving maneuver, such as acceleration or a lane change maneuver. Moreover, it supports real-time energy consumption estimation without recording too many historical states. A real-time energy consumption indicator will be described in the next section. The energy consumption for the 8184 drivers is sorted and equally split into three levels: low, medium, and heavy energy usage. The equal splitting of energy consumption is essential so that a fair interclass performance comparison can be made.

The energy-aware driving behavior module statistically analyzes the longitudinal acceleration/deceleration behaviors and the lateral lane-change behaviors for each vehicle. The frequency and duration of the acceleration/deceleration behaviors are calculated. Similarly, the frequencies of lane-change behaviors being studied. Moreover, lane-change behaviors are direction-dependent, which means that left-lane-change and right-lane-change behaviors are also studied. Then, the SSD test will be proposed for each car to assess the smoothness of motion behavior (trajectory and velocity).

The PJTSM approach is applied for trajectory and velocity prediction. The PJTSM approach contains joint LSTM layers for temporal pattern extraction for the three different energy consumption levels. Then, personalized fully connected (FC) regressors will be built for each class to precisely estimate future motion. Finally, based on the motion prediction for the three energy consumption levels, the interclass performance will be proposed to investigate the differences in the prediction for each energy consumption behavior. This section will provide a straightforward perspective on the relationship between energy usage behaviors and motion prediction performance. The results will benefit the design of intelligent traffic context-aware systems for future CAVs.

III. Energy-Aware Driving Pattern Analysis and Recognition

In this section, the energy-aware driving behaviors based on the NGSIM of a naturalistic highway dataset are investigated. The longitudinal acceleration/deceleration and lateral lane-change behaviors are statistically analyzed. Then, the smoothness of the motion behavior considering different energy usage levels is evaluated.

A. Energy Consumption Calculation and Classification

In this part, the energy consumed by each vehicle is calculated based on a simplified estimation of the required mechanical energy at the wheel [49]. A real-time energy consumption indicator (RT-ECI) is calculated for the average mechanical energy required at the wheel based on the vehicle dynamics every three seconds. The RT-ECI enables the real-time estimation of the energy consumption of CAVs and the selection of personalized predictors for motion prediction. To increase the computational efficiency, the RT-ECI will be calculated with a sliding window method. The RT-ECI is calculated every three seconds with the three seconds interval and can be represented as a function of the average velocity and acceleration in (1). Then, the mean RT-ECI for each trip is calculated in (2).

$$E_i = \frac{1}{3600}[mass \cdot g \cdot (f \cdot cos\varphi + sin\varphi) + 0.0386 \cdot A \cdot V_i{}^2 + mass \cdot ACC_i] \quad (1)$$

$$E_{mean} = \frac{\sum_{i=1}^{N} E_i}{N} \quad (2)$$

where E_i is the estimated energy consumption for each three-second segment and E_{mean} is the mean energy consumed during the whole trip; $mass$ is the total vehicle mass in kg. As the NGSIM data only provide vehicle types, the weight is roughly selected based on the average standards. Hence, an average of 2000 kg is selected in this study. g is the gravitation acceleration in 10 m/s^2. f is the rolling resistance coefficient of the vehicle, which is assumed to be 0.014, φ is the road gradient angle in degrees, which is selected as 0° in this study as the NGSIM data are mainly collected on flattened highway areas, and no hill was assumed in this part. A is the vehicle equivalent cross-section in m^2, which is roughly selected as 3 m^2. V is the average velocity in km/h for every three seconds, and ACC is the average acceleration in m/s^2. The RT-ECI will be used to indicate the real-time energy consumption level of the vehicle and help the personalized neural network for future motion prediction. The detailed process will be described in the next section.

B. Longitudinal Driving Behavior Analysis

In this part, the longitudinal driving behaviors are statistically analyzed considering different energy consumption levels. All the features used to analyze the driving behaviors are listed in Table 1. The maximum, minimum, mean, and standard deviation (SD) of the vehicle states are generated. The statistics of the selected longitudinal driving behaviors are listed in Table 2. As shown in Table 2, there are significant differences among the different energy consumption levels for most of the features except deceleration. Specifically, the heavy energy users tend to generate higher speeds and accelerations, larger space headways, and maintain less time headway with the leading vehicle. However, no obvious patterns exist in deceleration behaviors. The statistics of the longitudinal driving behaviors based on the RT-ECI show consistent results with the results in [49], which were achieved using the whole-trip energy consumption indicator.

As acceleration and deceleration behaviors are essential to energy consumption, the two behaviors will be further analyzed by considering the frequency and duration of these two maneuvers. Two metrics are used to describe the acceleration, constant, and deceleration behaviors for different energy consumption levels. The mean frequency of each maneuver is calculated with (4), where the time unit is one second. The percentage of each maneuver is calculated in (5) to measure the

proportion of the duration of each maneuver during the whole trip.

$$MFreq_s = \frac{N_S}{F} \times 10 \quad (3)$$

$$Perct = \frac{F_S}{F} \quad (4)$$

where $MFreq_s$ is the mean frequency of each stage (acceleration, constant, and deceleration), N_s is the total number of cases for each stage, F is the total number of frames, $Perct$ is the percentage of each stage, and F_s represents the total number of frames for each stage in the trip.

TABLE 1
STATISTICS OF THE FEATURES USED FOR DRIVING STYLE RECOGNITION

Feature	Statistics	
Speed (SPD) [km/h]	Max Speed	Min Speed
	SD of the Speed	Mean Speed
Acceleration (ACC) $[m/s^2]$	Max Acceleration	Mean Acceleration
	SD of the Acceleration	
Deceleration (DEC) $[m/s^2]$	Max Deceleration	Mean Deceleration
	SD of the Deceleration	
Space Headway (SH) [m]	Max Space Headway	Min Space Headway
	SD of the SH	Mean Space Headway
Time Headway (TH) [s]	Max Time Headway	Min Time Headway
	SD of the TH	Mean Time Headway

TABLE 2
COMPARISON OF THE KEY PARAMETERS OF THE DIFFERENT DRIVING STYLES AND ENERGY CONSUMPTION LEVELS

PARAMETER	SPD MAX	SPD MIN	SPD SD	SPD MEAN	ACC MAX	ACC SD	ACC MEAN	DEC MAX	DEC SD
LIGHT	43.689	5.136	9.157	**22.214**	3.456	1.154	**1.205**	3.456	1.157
MEDIUM	53.793	11.967	10.706	**31.857**	3.456	1.141	**1.240**	3.456	1.132
HEAVY	70.278	30.160	10.364	**48.765**	3.456	1.154	**1.378**	3.456	1.137
PARAMETERS	**DEC MEAN**	**SH MAX**	**SH MIN**	**SH SD**	**SH MEAN**	**TH MAX**	**TH MIN**	**TH SD**	**TH MEAN**
LIGHT	**1.223**	34.163	6.720	6.090	**16.502**	9.277	0.978	1.443	**3.194**
MEDIUM	**1.196**	38.639	8.529	7.187	**20.195**	6.992	0.966	1.064	**2.633**
HEAVY	**1.250**	48.690	11.637	9.200	**26.655**	3.968	0.986	0.637	**2.084**

TABLE 3
STATISTICS OF THE ACCELERATION-DECELERATION BEHAVIORS OF CAR USERS

A-D Statistics	Light	Medium	Heavy
Frequency of Accelerations	0.796	0.826	0.914
Percentage of Accelerations	30.23%	32.86%	39.48%
Frequency of Constant Speeds	0.579	0.714	0.716
Percentage of Constant Speeds	37.93%	34.39%	25.10%
Numbers of Decelerations	0.802	0.835	0.930
Percentage of Decelerations	31.23%	32.11%	34.52%

The statistics of the three longitudinal maneuvers are shown in Table 3. It is clear that both the frequency and duration of the maneuvers are significantly different among the three energy consumption levels. Specifically, heavy energy users tend to switch maneuvers more frequently than the drivers in the other two groups. Moreover, the duration of the acceleration and deceleration maneuvers of the heavy energy users is much longer than that of the drivers in the other two groups, while the constant speed duration is significantly shorter.

C. *Lateral Driving Behavior Analysis*

In this part, the lateral lane change driving behaviors are analyzed regarding the three energy consumption levels. Specifically, three lane-change metrics, namely, the overall lane-change frequency, left-lane-change frequency, and right-lane-change frequency, are calculated. The time scale of the lane-change frequency is also three seconds, which is the same as the RT-ECI. The three metrics are calculated as follows.

$$LC = \frac{N_{lc}}{T} \times 3 \quad (5)$$

$$LLC = \frac{N_{LLC}}{T} \times 3 \quad (6)$$

$$RLC = \frac{N_{RLC}}{T} \times 3 \quad (7)$$

where LC, LLC, and RLC are the 3-second rates of total lane changes, left lane changes, and right lane changes, respectively. N_{lc}, N_{LLC}, and N_{RLC} are the number of the lane-change behaviors, and T is the time duration of the whole trip.

TABLE 4
COMPARISON OF THE KEY PARAMETERS OF LANE-CHANGE BEHAVIORS AND SMOOTHNESS OF THE MOTION BEHAVIORS

PARAMETER	LC MAX	LC SD	LC MEAN	LLC MAX	LLC SD	LLC MEAN	RLC MAX	RLC SD	RLC MEAN
LIGHT	3.246	0.401	**0.188**	2.912	0.372	**0.159**	1.323	0.117	**0.029**
MEDIUM	4.268	0.490	**0.223**	3.658	0.434	**0.180**	2.581	0.191	**0.043**
HEAVY	7.167	0.961	**0.464**	6.360	0.692	**0.284**	3.389	0.525	**0.179**
PARAMETERS	**SSM MAX**	**SSM MIN**	**SSM SD**	**SSM MEAN**	**TSM MAX**	**TSM MIN**	**TSM SD**	**TSM MEAN**	
LIGHT	3.711	0.744	0.481	**1.983**	2.881	0.692	0.295	**1.533**	
MEDIUM	5.248	1.512	0.568	**2.875**	3.851	1.065	0.325	**1.990**	
HEAVY	8.044	2.557	0.735	**4.455**	6.629	1.791	0.472	**2.841**	

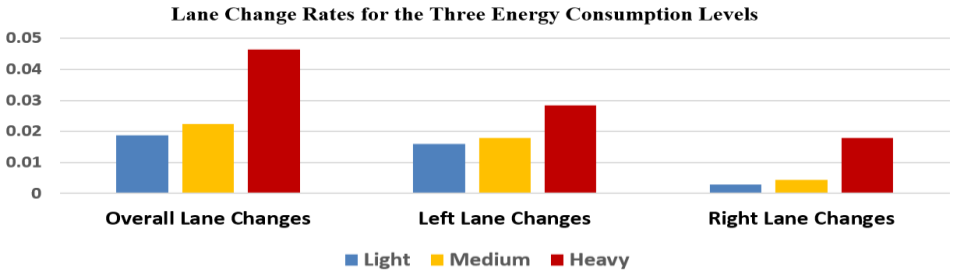

Fig. 3. Bar plots of the 3-second mean lane-change rates considering the three energy consumption levels.

The statistical results of the lane-change maneuvers are shown in Table 4 and Fig. 3. Consistent results are achieved for the three metrics. Fig. 3 shows the mean frequency of the three lane-change maneuvers considering different energy consumption levels. It is clear that the heavy energy users will also generate more lane change (including both left-lane-change and right-lane-change) maneuvers than the low and medium energy users.

D. Smoothness Analysis of the Motion Behaviors

In this part, the smoothness of the motion behaviors (i.e., vehicle velocity and trajectory) is evaluated using the sliding standard deviation test. The reason for proposing the SSD test is to exploit further the patterns in energy-aware driving behaviors. The motion behaviors (i.e., velocity and trajectory) are the most straightforward observations of the surrounding vehicles. The SSD test enables the smoothness and regularity evaluation of these motion behaviors. A higher SSD index (SSDI) represents higher randomness, and variation exists in the signals, which could be more difficult to predict. A smaller SSDI means that the signal is smoother and more predictable. The sliding window test uses a sliding window to calculate the standard deviation of the sliding slice, and then the average SD of the whole signal will be statistically analyzed based on the SSD of these segments.

A nonoverlapped sliding window method is used to increase computational efficiency. The sliding window size in this study is selected as 10 data points, which is a one-second segment. The SSDI of the smoothness of the whole steering period can be represented as the mean SD of the whole sliding slices of each sequence.

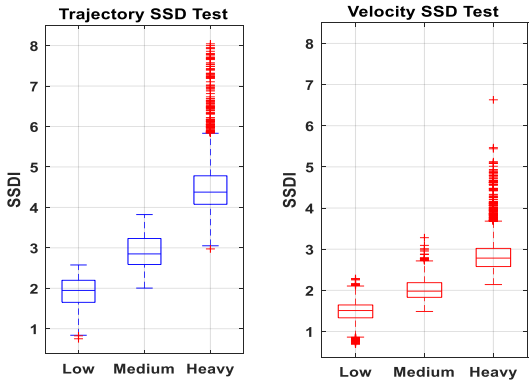

Fig. 4. Boxplot of the sliding standard deviation test for the trajectory and velocity states considering different energy consumption levels. The x-axis represents the three energy consumption levels, and the y-axis is the value of the SSDI.

$$SSDI = \frac{1}{N}\sum_{N}\sqrt{\frac{\sum_{m=1}^{M}(x_m-\mu_M)^2}{M}} \quad (8)$$

where N is the total number of sliding slices of the whole sequence, M is the selected window size for each slice, x_m is the m[th] point within the segment, and μ_m is the mean value of this segment. The joint trajectory of the vehicle is calculated as follows.

$$Traj_i = \sqrt{{x_i}^2 + {y_i}^2} \quad (9)$$

where $Traj_i$ is the track of the i[th] point and x_i and y_i are the lateral and longitudinal position points, respectively, in the dataset.

The size of the sliding window is 10 points, which is small enough to evaluate the stability and variation in each slice smoothly. It should be noted that a sliding window size that is too large cannot efficiently measure the local smoothness of the steering torque, which can lead to a coarse statistical result. However, the size of the sliding window cannot be too small, as such a window can only provide short period variations and is unable to measure the dynamic trends and significant variations among the signals. The statistical results of the measured SSDIs for the vehicle velocity and trajectory are shown in Table 4 and Fig. 4. Consistent results are found in the boxplots in Fig. 4; vehicles with higher energy consumption tend to generate a higher SSDI, which means that the variation and randomness in the trajectory and velocity states are larger than those of vehicles with lower energy consumption.

IV. Model Construction

In this section, the PJTSM network construction and training process are introduced. The PJTSM network is trained with the NGSIM dataset. Specifically, the US-101 and I-80 freeway driving data are used. Only the leading vehicle is considered to simplify the analysis and gain a first perspective on the relationship between energy consumption and motion prediction, and the sophisticated interaction behaviors with surrounding vehicles are not considered. In total, 5574 following-leading naturalistic driving data points are extracted with interaction durations longer than six seconds. The model takes the historical motion data of the leading vehicle as input and outputs the predicted trajectory and velocity states. As shown in existing studies, the prediction error of the surrounding vehicle mainly comes from the longitudinal position [30,43]. In the following analysis, the joint trajectory described in (9) will be used for simplicity. The simplified PJTSM network can be represented as follows.

$$Y_{t+n} = PJTSM(X_{1:t}) \quad (10)$$

$$X = \{X_{spd}, X_{acc}, X_{pos}, X_{sh}, X_{th}\} \quad (11)$$

where the output Y is the predicted trajectory and velocity sequence, and n is the prediction horizon; one- to five-second prediction horizons are used in this study. The sequential input data are a set of a series of leading vehicle states. The input vehicle states are shown in Table 5.

TABLE 5
Selected Sequential Features for Model Training

Features	Sequential Inputs
Speed	Max Speed, Min Speed, Mean Speed, SD of the Speed
Acceleration	SD of the Acceleration, Mean Acceleration
Space Headway	Max Space Headway, Mean Space Headway
Time Headway	Max Time Headway, Mean Time Headway

The model training contains two separate stages: joint sequential model training and personalized prediction network fine-tuning. Before training the common sequential model, 80% of the whole dataset is used as training data, while the remaining 20% of the data are used for model testing. The joint sequential model contains two LSTM layers, as shown in Fig. 1. Each of the LSTM layers has 120 LSTM cells. The two fully connected (FC) layers of the PJTSM model have 300 and 30 neurons. The training and testing datasets are equally divided into three groups according to the corresponding energy consumption levels. The personalized networks are also

defined based on energy consumption levels. For different driving behaviors and energy consumption levels, a specific prediction network is built so that the model can generate personalized predictions for each group. The three personalized prediction networks follow the same structure of the joint sequential model, except the FC layers are fine-tuned using the subdataset. The sizes of the two FC layers of the personalized prediction network are reduced to 150 and 10 neurons to increase the computational efficiency and avoid overfitting. The networks are developed with MATLAB 2019b.

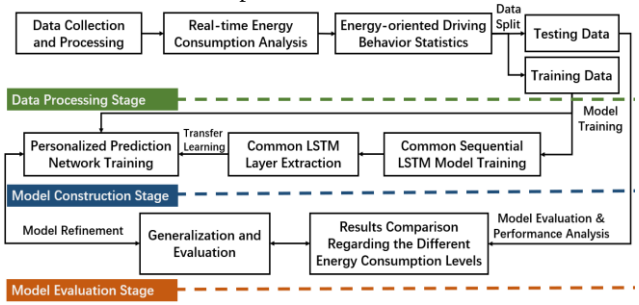

Fig.5. Illustration of the construction process of the PJTSM model.

The detailed training and testing processes are illustrated in Fig. 5 below. The testing data are only used for model testing and evaluation to prevent data leakage issues. The construction of the personalized joint time-series model can be divided into three stages. First, in the data processing stage, the naturalistic driving data from the NGSIM dataset is collected. The energy consumption and the energy-oriented driving behaviors for the vehicles are analyzed. In the second stage, the model is constructed based on sequential LSTM and RNN networks. The joint temporal pattern extraction layer (with two LSTM layers) for the three groups will be trained with the whole training dataset. Regarding the personalized prediction networks, the two LSTM layers are extracted for temporal feature extraction. Then, three separate FC-based prediction layers are designed for each energy consumption level. Last, in the model evaluation stage, the general model prediction accuracy for the trajectory and velocity will be first evaluated. Then, the prediction accuracy regarding different energy consumption levels will then be evaluated.

The joint sequential model is trained with Adam optimizer with a learning rate of 0.01. The maximum number of epochs is 150, and the mini-batch size is 32. Regarding the personalized prediction models, the sequential LSTM layers of the joint model are adopted with an initial learning rate of 0.0001 to slow down the learning in the transfer layer, while the weighted learning rate of the FC layer is 20 to speed up the learning process of the new layers. The maximum epoch of the personalized networks is 120.

V. Experimental Results

In this section, the experimental results and model evaluation metrics are discussed. The PJTSM approach to motion prediction is compared with several baseline methods. Then, the prediction accuracy considering the different energy usage levels is investigated.

A. Baselines and Evaluation Metrics

In this section, the baseline algorithms and the evaluation metric for the evaluation of vehicle states are described. The root-mean-square error (RMSE) is calculated to evaluate the prediction performance. Moreover, the mean RMSE for the worst 1% and 5% cases are reported to assess further the algorithm performance under critical situations. The RMSE can be calculated as follows.

$$RMSE(v) = \sqrt{\frac{1}{N}\sum_{i=1,2,\cdots N}((\hat{x}_i - x_i)^2)} \qquad (12)$$

where v is the vth vehicle, N is the total number of points in the historical horizon, and $\hat{x}_i$ and x_i are the predicted value and the ground-truth value, respectively.

Several baselines are used to perform a comparison among the existing algorithms and proposed methods. The baselines are as follows:

1. **LR**. A linear regression model is used, as vehicle motion is usually not very complex.
2. **FFNN**. A conventional multilayer perceptron feedforward neural network (FFNN) model is trained to predict the vehicle states. Fifty neurons are selected in the hidden layer.
3. **S-LSTM**. A single LSTM-RNN model is trained to predict the sequential vehicle states without considering different energy consumption levels. The SLSTM model has two LSTM layers following with two FC layers for sequential prediction. The SLSTM has the same structure as the joint sequential model, as developed in the first stage of the PJTSM.
4. **MLSTM**. A multiple-LSTM method is used to train a separate LSTM based RNN network for each class, and three LSTM networks are trained with the subdataset from the specific group. Each of the MLSTM models has the same structure as the PJTSM, with two LSTM layers and two FC layers.
5. **PJTSM**. The personalized joint time-series model is built based on the common temporal feature extraction layer and personalized regression layers. The common temporal layer has two LSTM layers (each layer has 120 LSTM cells). Each of the three FC networks has two FC layers, with 150 and 10 neurons, respectively.

In sum, the discriminative models like LR and FFNN models can generate instant prediction results for the trajectory and velocity, which can be used to assess the advantages of the sequential networks. The S-LSTM model has similar sequential pattern extraction layers with the PJTSM model, following with one uniform FC network. The S-LSTM model can be used to evaluate the efficiency of the personalized prediction for the vehicle states. The M-LSTM models have similar structures to the personalized prediction network but do not share the common temporal pattern extraction layers. The M-LSTM model can be used to assess the advantages of the joint time-series modeling approach.

B. Prediction of the Trajectory and the Velocity States

The prediction results for the trajectory and velocity states based on the different baseline methods are described in this part. The primary consideration of using the PJTSM model is to train a joint temporal extraction layer based on the whole

dataset so that the common LSTM layer can capture the temporal patterns as much as possible. The trajectory prediction results are shown in Table 6.

TABLE 6
COMPARISON OF THE TRAJECTORY PREDICTION RESULTS

	Metrics	LR	FFNN	S-LSTM	M-LSTM	PJTSM
1 s	RMSE	3.547	3.431	0.678	1.785	0.516
	Top 5%	20.406	19.612	1.755	4.504	1.632
	Top 1%	31.026	29.630	3.878	6.863	3.020
2 s	RMSE	3.997	3.840	1.699	2.422	1.329
	Top 5%	23.123	22.452	3.498	6.058	3.143
	Top 1%	34.074	34.529	5.282	8.479	4.979
3 s	RMSE	4.316	4.154	2.621	2.989	2.283
	Top 5%	24.349	23.986	7.339	8.133	6.390
	Top 1%	35.225	36.208	15.321	14.472	12.619
4 s	RMSE	4.648	4.463	3.289	3.788	2.884
	Top 5%	26.947	25.428	10.528	11.069	8.836
	Top 1%	39.863	36.956	18.410	17.530	15.976
5 s	RMSE	4.865	4.713	3.861	4.372	3.492
	Top 5%	28.062	27.454	12.165	12.887	10.473
	Top 1%	41.019	42.140	18.888	20.441	17.659

As shown in Table 6, the PJTSM network achieved the most accurate results with different prediction horizons. The performance of the basic S-LSTM is better than that of the MLSTM model, which shows the efficiency of the common temporal LSTM layer. The linear regression model and the FFNN model achieved significantly higher RMSEs than the time-series models, indicating the sequential time-series models are more advantage than the discriminative models. The RMSEs of the PJTSM is 0.516 m and 2.884 m with a one-second and four-second prediction horizon, respectively. The RMSE of the PJTSM becomes 3.492 m with a five-second prediction horizon, which is a relatively large error and shows that it is less likely to achieve a precise prediction in real time with such a larger prediction horizon. Moreover, the worst 1% of the results with a three-second horizon increase dramatically to more than 10 m for the three deep learning-based approaches, which shows that it would be better to make track predictions within three seconds in real time than for the other time periods. An exemplar illustration of the track prediction is shown in Fig. 6, which shows that the bias between the prediction results and the ground-truth track of the PJTSM network is the smallest among the three methods.

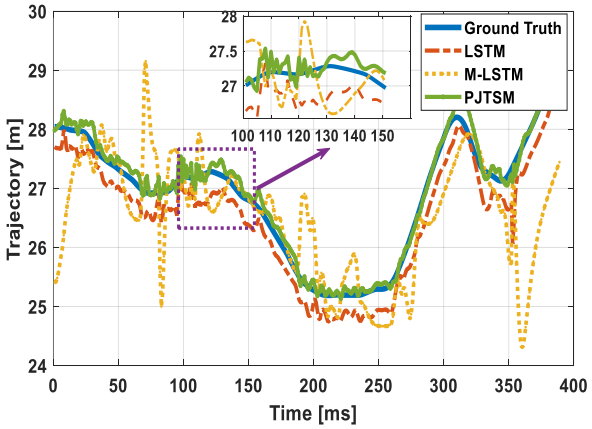

Fig. 6. Example illustration of the trajectory prediction results of different algorithms with the prediction made one second ahead.

TABLE 7
COMPARISON OF THE VELOCITY PREDICTION RESULTS

	Metrics	LR	FFNN	S-LSTM	M-LSTM	PJTSM
1 s	RMSE	6.387	5.926	1.765	3.215	1.581
	Top 5%	25.016	24.138	3.593	6.509	3.481
	Top 1%	30.582	30.630	4.952	7.908	4.910
2 s	RMSE	7.073	6.628	3.385	4.488	3.328
	Top 5%	27.013	26.698	8.073	8.385	7.480
	Top 1%	33.253	36.605	11.934	11.070	10.777
3 s	RMSE	7.699	7.427	4.726	5.634	4.147
	Top 5%	28.608	28.105	10.566	10.238	9.724
	Top 1%	34.391	34.536	17.618	15.151	16.694
4 s	RMSE	8.210	8.064	5.610	6.475	5.056
	Top 5%	29.815	29.297	12.608	11.856	11.147
	Top 1%	36.045	35.608	17.811	16.457	16.056
5 s	RMSE	8.682	8.405	7.248	7.389	6.034
	Top 5%	30.683	30.430	15.358	13.946	13.933
	Top 1%	36.576	37.160	21.197	18.644	21.043

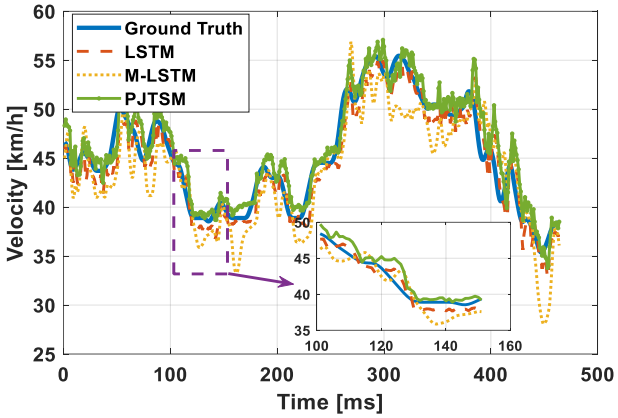

Fig. 7. Example illustration of the velocity prediction results of different algorithms with the prediction made one second ahead.

The velocity prediction results are shown in Table 7 and Fig. 7. Similar to the track prediction results, the PJTSM network achieved the most precise prediction results with different prediction horizons. The mean RMSE for the one-second prediction horizon is 1.581 km/h, and the top 1% and top 5% RMSEs are 4.910 km/h and 3.481 km/h, respectively. Although the mean RMSE does not significantly increase by increasing the prediction horizon, the top 1% and top 5% prediction results increase dramatically. The top 1% RMSE of the PJTSM network with a three-second prediction horizon increased to 16.694 km/h, which is a large prediction error for a real-time velocity predictor. Hence, to maintain a reasonable prediction accuracy, a similar selection of the prediction horizon (within three seconds) with track prediction is needed.

In sum, based on the results from Table 6 and Table 7, and the prediction comparison for different methods shown in Fig. 6, and Fig. 7, it can be found that the proposed PJTSM approach always leads to the most accurate results, which show the efficiency of the personalized prediction and joint time-series modeling. The other two sequential networks (S-LSTM and M-LSTM) focus on different aspects. Specifically, the S-LSTM focuses on the joint time-series model, while the M-LSTM focus on personalized training. It is shown that the S-LSTM model can generate better prediction performance compared to the M-LSTM models. The reasons can be multi-fold. First, the S-LSTM model is trained more training data than the M-LSTM models, which can capture

more temporal patterns. Due to the less training data, underfitting can occur for the M-LSTM model, which leads to the large prediction error and the high variance. By comparing the PJTSM model with these two models, it can be found that the two-stage model training process can further improve the system performance.

C. *Performance Comparison Among the Different Groups*

In this part, the differences in the trajectory and velocity prediction regarding the different energy consumption levels are analyzed further to exploit the characteristics of different energy-aware driving behaviors. As mentioned above, the acceleration/deceleration and lane-change behaviors are highly correlated with energy consumption. It is necessary to evaluate the relationship between driving behaviors and motion prediction so that a precise prediction model can be designed.

TABLE 8
COMPARISON OF THE TRAJECTORY PREDICTION RESULTS CONSIDERING THE DIFFERENT ENERGY CONSUMPTION LEVELS

	Horizon	1 s	2 s	3 s	4 s	5 s
PJTSM	Low	0.351	1.092	1.778	2.282	2.772
	Medium	0.499	1.216	1.993	2.633	3.356
	Heavy	0.697	1.678	3.079	3.738	4.348
LSTM	Low	0.601	1.208	1.767	2.547	3.020
	Medium	0.695	1.336	2.116	3.121	3.530
	Heavy	0.735	2.555	3.979	4.200	5.032

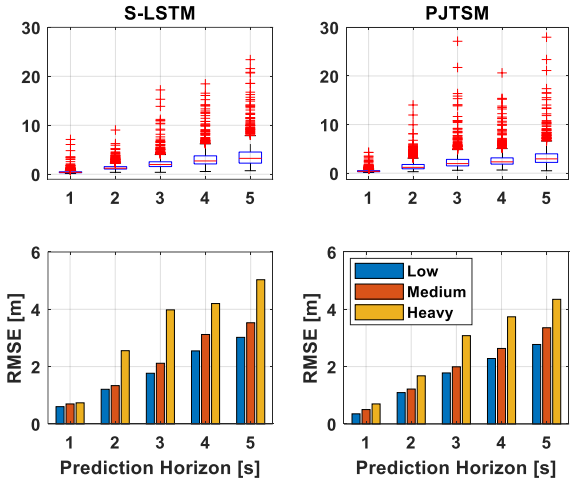

Fig. 8. Statistical results of the trajectory prediction results using the S-LSTM and PJTSM methods. The upper two boxplots show the statistical RMSE results regarding different prediction horizons. The bottom bar charts show the mean trajectory RMSEs for the different energy consumption levels regarding different prediction horizons.

The comparison of the trajectory prediction results between the PJTSM and S-LSTM networks considering different energy consumption levels is illustrated in Table 8 and Fig. 8. Consistent patterns exist between these two algorithms. Specifically, track prediction for cars exhibiting heavy energy consumption is the most difficult and leads to the largest RMSE with both algorithms. With the same model and the same number of training data, the heavy energy consumption behaviors always show larger RMSE results than the lower energy consumption group with different prediction horizon. In contrast, the track prediction for cars with low energy consumption is more precise than that of the other two groups. Based on the driver behavior analysis, it can be found that frequently performing lane-change maneuvers (heavy energy driving behaviors) and acceleration/deceleration maneuvers will make the driving behavior highly random and increase the difficulty of precise track prediction. Therefore, for the future design of automated driving vehicles, it is recommended to design smooth automated driving strategies to avoid a frequent change of lateral and longitudinal maneuvers to decrease the energy consumption, improve the behavior understanding ability, and enable efficient interactions between different entities.

The RMSE statistics for the trajectory prediction analysis are illustrated in Fig. 8. The boxplots in the upper row show the statistical prediction results of the two algorithms. Based on the upper two graphs of Fig.8, it is shown that the distribution of the RMSE for two methods does not show a significant difference. Based on the bottom two graphs of Fig. 8, it is shown that although the PJTSM network generates a larger standard deviation in some cases, the mean accuracy is higher than that of the S-LSTM method. Based on the mean RMSE of each group in the bottom bar charts, it can be found that the personalized networks can efficiently reduce the prediction RMSE as well as the differences among the groups.

Similar results and consistent patterns among the three groups can be found in the velocity prediction case. Based on the velocity prediction results shown in Table 9 and Fig. 9, it can be found that the velocity prediction for the cars exhibiting heavy energy consumption is also the least accurate among the three groups. As discussed earlier, heavy energy consumption behaviors usually lead to frequent and longer acceleration and deceleration processes. These longitudinal behaviors, as well as the frequent lane-change maneuvers, also contribute to the higher prediction error of the vehicle velocity.

TABLE 9
COMPARISON OF THE VELOCITY PREDICTION RESULTS CONSIDERING THE DIFFERENT ENERGY CONSUMPTION LEVELS

	Horizon	1 s	2 s	3 s	4 s	5 s
PJTSM	Low	1.424	2.928	3.832	4.738	5.639
	Medium	1.546	3.154	3.969	5.161	6.081
	Heavy	1.792	4.180	4.794	5.448	6.570
LSTM	Low	1.505	3.209	4.753	5.173	6.987
	Medium	1.745	3.244	4.564	5.532	7.263
	Heavy	2.043	3.530	4.861	6.125	7.494

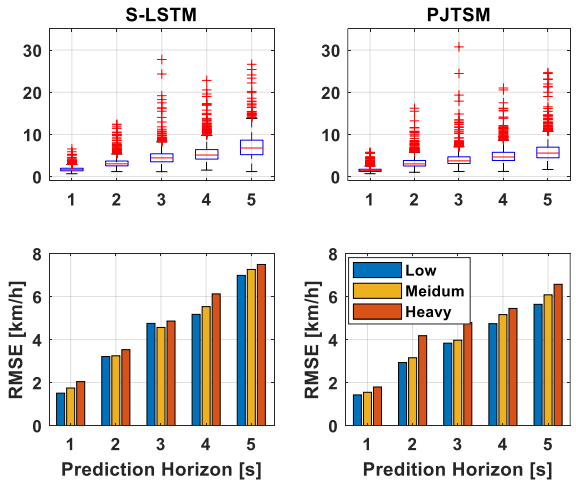

Fig. 9. Statistical results of the velocity prediction results using S-LSTM and PJTSM methods. The upper two boxplots show the statistical RMSE results regarding different prediction horizons. The bottom bar charts show the mean RMSEs for the speeds at different energy consumption levels regarding different prediction horizons.

The statistics of the velocity prediction results are shown in Fig. 9. Unlike the large differences in the prediction results in the trajectory prediction case, the differences in the velocity prediction are less substantial. Applying the PJTSM approach can also increase the velocity prediction accuracy compared to the S-LSTM approach. Although in some cases, the prediction error for the low energy consumption cars is slightly larger than the medium class using the LSTM network, the overall trend is similar to that of the track prediction analysis that the cars exhibiting heavy energy consumption usually generate a higher velocity prediction RMSE than the other types of cars. Based on the analysis and comparison shown in Fig.8 and Fig. 9, it can be found that heavy energy consumption-oriented driving behaviors can also lead to higher prediction error in the vehicle trajectory and velocity prediction, and vice versa. Hence, it can be concluded that the energy consumption level can be connected to the vehicle state prediction based on energy-aware driving behaviors.

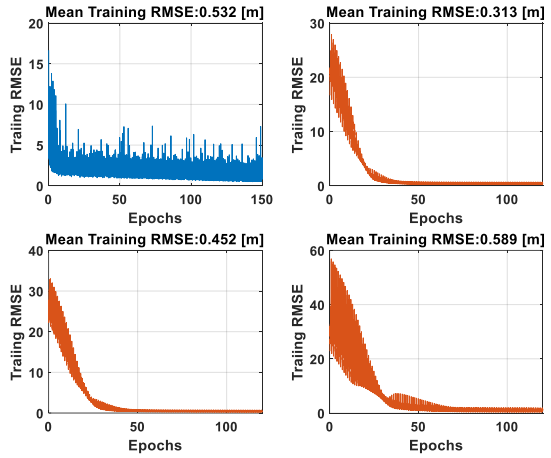

Fig. 10. The training process and training RMSE visualization for the S-LSTM and PJTSM models. The first graph with the blue line shows the training process for the S-LSTM model; the rest three graphs with the red lines are the training results for the low, medium, and heavy energy consumption group for the trajectory prediction task

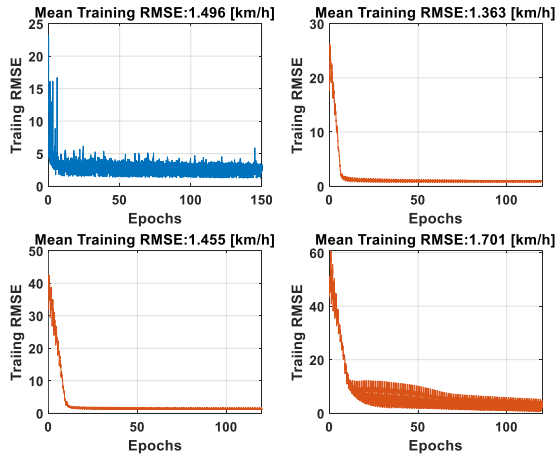

Fig. 11. The training process and training RMSE visualization for the S-LSTM and PJTSM models. The first graph with the blue line shows the training process for the S-LSTM model; the rest three graphs with the red lines are the training results for the low, medium, and heavy energy consumption group for the velocity prediction task.

The training process and training RMSE of the S-LSTM and PJTSM for the trajectory and velocity prediction is illustrated in Fig. 10 and Fig.11, respectively. From these two graphs, it can be concluded that with the fine-tuning method, the training process of the PJTSM model (shown in the red lines) is smoother than that in the S-LSTM training case. The PJTSM can converge much faster than the S-LSTM model dues to the fine-tune scheme to the final FC layers. From the PJTSM model training process, it can be found that the training data from the different energy consumption groups lead to different training progress in terms of accuracy and convergency. Specifically, for both of the trajectory and velocity prediction cases, the average training RMSE of the low energy consumption group is also the smallest among the three groups, and the training process is much smoother than the other two groups. Moreover, the low energy consumption model is easier to be converged than the other two groups dues to the well predictable driving behaviors.

VI. Discussion and Future Works

In this study, the energy consumption of each vehicle is measured based on an energy consumption indicator. This approach measures the real-time energy consumption so that the energy consumption label can be used for real-time motion prediction. This approach is more efficient than that in [50], which calculated the energy consumption over a whole trip or a certain distance. Although the ECI has no real unit, this is not a critical issue, as the primary motivation of adopting the ECI is to find different energy consumption levels so that the corresponding driving behaviors can be further determined.

A. Discussion

1) Influential Factors to Vehicle Motion Prediction

Based on the energy-aware analysis, we found that significantly different patterns exist among the three energy consumption levels. It is shown that the average driving speed and space headway of heavy energy usage cars are much larger than cars at the medium and low energy consumption levels, while the time headway is much shorter. These results are consistent with the results in [50]. Regarding longitudinal driving behaviors such as acceleration, deceleration, and constant speeds, heavy energy users will spend 39.48% and 34.52% of the driving duration accelerating and decelerating, respectively, while they maintain a constant speed only 25.1% of the time, which is much lower than that in the low energy consumption group (37.9%). Similar results and conclusions can be drawn from the statistics of the lateral lane-change behaviors. Specifically, the overall lane-change frequency of the cars exhibiting heavy energy usage is much larger than that of the cars with low energy consumption. This finding shows that both the longitudinal and lateral driving behaviors for different energy consumption levels are significantly different from each other, which shows a highly correlated relationship between energy consumption and driving behaviors.

The differences in the driving behaviors for the different energy consumption groups can be further reflected by the trajectory and velocity prediction results using the PJTSM network. Based on the statistical results of the trajectory and velocity prediction analyses, consistent patterns are found. The

prediction accuracy is dependent on the energy-aware driving behaviors. For heavy energy consumption cars, their future tracks and speeds are more difficult to predict due to the more frequent acceleration/deceleration and lane-change maneuvers. Moreover, it is found that the prediction accuracy can be improved while the differences in the prediction results among the three groups can be decreased using the PJTSM approach. This finding shows the efficiency and necessity of using a personalized modeling method for different traffic objects. However, this approach could raise another problem, which is how to select the proper number of groups for traffic context understanding. As shown in Fig. 8 and Fig. 9, the differences within the prediction results of the low and medium energy consumption groups are not as significant as those of the heavy energy consumption group. Therefore, two groups may be sufficient to describe energy-aware driving behaviors in the future.

2) Contribution to the Safety Applications in Transportation Systems

The analysis of vehicle energy consumption-oriented driving styles and vehicle motion prediction system will further contribute to developing safe transportation systems in the future. The vehicle motion prediction is closely related to vehicle interaction for intelligent vehicles. Reasonable decisions and planning strategies can be made with surrounding vehicle motion prediction and evaluation, which will then contribute to more efficient and safer real-world interactions between the future intelligent and automated vehicles. In general, the proposed system will benefit the future design of safe transportation systems in three aspects. First, motion prediction enables the path planning algorithm to generate safer and efficient trajectories for the ego-vehicle to avoid conflicts with the surrounding vehicle. Second, integrating different driving behavior knowledge into the motion prediction contribute to a holistic understanding of the surrounding traffic context, which will enable safer interaction between different road users and the development of courtesy automated driving [51]. Last, the energy-oriented driving behaviors analysis and motion prediction model provides lead to an energy-efficient and sustainable smart transportation system by connecting the driving behaviors with the energy consumption [52].

B. Future Works

1) Improve Interaction-Aware Model for Precise Vehicle Motion Prediction

It should also be mentioned that in this study, the driving data of the leading and following cars are used for the construction of the energy-aware PJTSM network. With the leading-following interaction features and the personalized motion prediction network, the future trajectory and vehicle speed can be accurately predicted based on the observed history data of the connected vehicle. Based on the proposed method, the energy consumption behaviors, driving behaviors, and the motion behaviors of the leading vehicle can be jointly analyzed, which will contribute to a better understanding of the leading vehicle and safer interactions between the leading and following vehicles.

It is also important to exploit the complex interaction behaviors with the surrounding vehicles of the connected vehicles. As shown in [30-34], interaction-aware motion prediction can provide a model for understanding the comprehensive traffic context. Future works can be further extended to the design of interaction-aware and energy-aware personalized motion prediction networks. The PJTSM network can be extended to adaptively model the surrounding vehicle behaviors and generate a personalized prediction for the target vehicle. We believe that the interaction behaviors with the surrounding vehicles are also energy sensitive, which means that more sophisticated interaction patterns for different energy consumption vehicles can also be analyzed with a personalized modeling approach. Hence, future works will also focus on the exploration of the connection between complex interaction behaviors and energy consumption levels as well as driving behaviors.

2) Improve Energy Consumption Indicator and Driving Behavior Representation

The real-time energy consumption indicator, which is the foundation of energy-aware-driving behaviors analysis, can be further improved in the future. The RT-ECI used in this study relies on the velocity of the target vehicle, which can be easily observed in the real-world. While the energy consumption of the vehicles can be more accurately predicted if integrating vehicle dynamic information such as the transition dynamics of the powertrain and vehicle dynamic models. Basic vehicle information can be expected on future CAVs, which will benefit the design of more accurate vehicle states prediction systems to let the ego-vehicle better understand the surrounding road users. Meanwhile, the driving behaviors in this study are represented by typical longitudinal and lateral driving behaviors. Future works can further enrich and integrate more driving behaviors such as overtaking or other interaction behaviors and habits. Such joint and holistic analysis of the energy consumption, driving behaviors, and vehicle motion prediction will further increase the efficiency and safety of future intelligent transportation systems.

VII. CONCLUSION

In this study, an energy-aware driving behavior analysis and motion prediction system for safer automated driving is proposed. The connections between energy consumption, driving behaviors, and motion prediction are exploited. The main conclusions of this study can be summarized as follows.

- The energy consumption level is associated with the longitudinal and lateral driving behaviors in this study. It is found that for cars exhibiting heavy energy usage, the driving speed and the frequency of the acceleration and deceleration behaviors are significantly larger than those of the other two levels. Moreover, cars exhibiting heavy energy usage tend to perform more lane-change maneuvers than others.
- The smoothness of driving dynamics (i.e., the velocity and trajectory) is evaluated. It is shown that the vehicle states are less smooth, and the regularity is much lower for the cars exhibiting heavy energy consumption.
- The motion prediction method for vehicle trajectory and velocity is proposed based on the energy-aware PJTSM approach. The PJTSM network shows its efficiency and accuracy in the motion prediction of leading cars.

- Finally, the prediction accuracy for different energy consumption levels is studied and compared. It is shown that heavy energy consumption behaviors will lead to larger state prediction errors, which makes it more difficult to estimate future vehicle states precisely. Additionally, the PJTSM network will lead to fewer interclass differences, which shows the necessity of designing personalized traffic context reasoning systems.

REFERENCES

[1] Dey, Kakan Chandra, et al. "Vehicle-to-vehicle (V2V) and vehicle-to-infrastructure (V2I) communication in a heterogeneous wireless network–Performance evaluation." *Transportation Research Part C: Emerging Technologies* 68 (2016): 168-184.

[2] Li, Li, et al. "Intelligence testing for autonomous vehicles: A new approach." *IEEE Transactions on Intelligent Vehicles* 1.2 (2016): 158-166.

[3] Ghane, Soheila, et al. "Preserving privacy in the internet of connected vehicles." *IEEE Transactions on Intelligent Transportation Systems* (2020).

[4] Siegel, Joshua E., Dylan C. Erb, and Sanjay E. Sarma. "A survey of the connected vehicle landscape—architectures, enabling technologies, applications, and development areas." *IEEE Transactions on Intelligent Transportation Systems* 19.8 (2017): 2391-2406.

[5] Zhang, Yuanzhi, et al. "Real-time energy management strategy for fuel cell range extender vehicles based on nonlinear control." *IEEE Transactions on Transportation Electrification* (2019).

[6] Aramrattana, Maytheewat, et al. "Safety Evaluation of Highway Platooning Under a Cut-In Situation Using Simulation." *IEEE Transactions on intelligent transportation systems* (Print) (2018).

[7] Meseguer, Javier E., et al. "Assessing the impact of driving behavior on instantaneous fuel consumption." *2015 12th Annual IEEE Consumer Communications and Networking Conference (CCNC)*. IEEE, 2015.

[8] Wang, Wenshuo, Junqiang Xi, and Ding Zhao. "Driving style analysis using primitive driving patterns with Bayesian nonparametric approaches." *IEEE Transactions on Intelligent Transportation Systems* 20.8 (2018): 2986-2998.

[9] Van Mierlo, Joeri, et al. "Driving style and traffic measures-influence on vehicle emissions and fuel consumption." *Proceedings of the Institution of Mechanical Engineers, Part D: Journal of Automobile Engineering* 218.1 (2004): 43-50.

[10] Song, Ziyou, et al. "Simultaneous identification and control for hybrid energy storage system using model predictive control and active signal injection." *IEEE Transactions on Industrial Electronics* (2019).

[11] Malekian, Reza, et al. "Guest editorial: Introduction to the special issue on connected vehicles in intelligent transportation systems." *IEEE Transactions on Intelligent Transportation Systems* 19.7 (2018): 2301-2304.

[12] Song, Ziyou, et al. "The influence of driving cycle characteristics on the integrated optimization of hybrid energy storage system for electric city buses." *Energy* 135 (2017): 91-100.

[13] Jafari, Mehdi, et al. "Simulation and analysis of the effect of real-world driving styles in an EV battery performance and aging." *IEEE Transactions on Transportation Electrification* 1.4 (2015): 391-401.

[14] Ping, Peng, et al. "Impact of driver behavior on fuel consumption: classification, evaluation and prediction using machine learning." *IEEE Access* 7 (2019): 78515-78532.

[15] Meseguer, Javier E., et al. "Drivingstyles: a mobile platform for driving styles and fuel consumption characterization." *Journal of Communications and networks* 19.2 (2017): 162-168.

[16] Rangaraju, Surendraprabu, et al. "Impacts of electricity mix, charging profile, and driving behavior on the emissions performance of battery electric vehicles: A Belgian case study." *Applied Energy* 148 (2015): 496-505.

[17] Chen, Yuche, et al. "Data-driven fuel consumption estimation: A multivariate adaptive regression spline approach." *Transportation Research Part C: Emerging Technologies* 83 (2017): 134-145.

[18] Zhou, Quan, et al. "Cyber-physical energy-saving control for hybrid aircraft-towing tractor based on online swarm intelligent programming." *IEEE Transactions on Industrial Informatics* 14.9 (2017): 4149-4158.

[19] Guensler, Randall, et al. "Energy consumption and emissions modeling of individual vehicles." *Transportation Research Record* 2627.1 (2017): 93-102.

[20] Wang, Yiwei, et al. "Enabling Courteous Vehicle Interactions through Game-based and Dynamics-aware Intent Inference." *IEEE Transactions on Intelligent Vehicles* (2019).

[21] Lv, Chen, et al. "Driving-style-based codesign optimization of an automated electric vehicle: a cyber-physical system approach." *IEEE Transactions on Industrial Electronics* 66.4 (2018): 2965-2975.

[22] Paden, Brian, et al. "A survey of motion planning and control techniques for self-driving urban vehicles." *IEEE Transactions on intelligent vehicles* 1.1 (2016): 33-55.

[23] Lin, Patrick. "Why ethics matters for autonomous cars." *Autonomous driving*. Springer, Berlin, Heidelberg, 2016. 69-85.

[24] Lefèvre, Stéphanie, Dizan Vasquez, and Christian Laugier. "A survey on motion prediction and risk assessment for intelligent vehicles." *ROBOMECH journal* 1.1 (2014): 1.

[25] Hillenbrand, Jrg, Andreas M. Spieker, and Kristian Kroschel. "A multilevel collision mitigation approach—Its situation assessment, decision making, and performance tradeoffs." *IEEE Transactions on intelligent transportation systems* 7.4 (2006): 528-540.

[26] Hongyan Guo, Chen Shen, Hui Zhang, Hong Chen, Rui Jia. Simultaneous Trajectory Planning and Tracking Using an MPC Method for Cyber-Physical Systems: A Case Study of Obstacle Avoidance for an Intelligent Vehicle. *IEEE Transactions on Industrial Informatics*, 14(9): 4273-4283, 2018, 9.

[27] Ortiz, Michaël Garcia, et al. "Behavior prediction at multiple time-scales in inner-city scenarios." *2011 IEEE Intelligent Vehicles Symposium (IV)*. IEEE, 2011.

[28] Morris, Brendan, Anup Doshi, and Mohan Trivedi. "Lane change intent prediction for driver assistance: On-road design and evaluation." *2011 IEEE Intelligent Vehicles Symposium (IV)*. IEEE, 2011.

[29] Bahram, Mohammad, et al. "A combined model-and learning-based framework for interaction-aware maneuver prediction." *IEEE Transactions on Intelligent Transportation Systems* 17.6 (2016): 1538-1550.

[30] Deo, Nachiket, and Mohan M. Trivedi. "Multi-modal trajectory prediction of surrounding vehicles with maneuver-based LSTM." *2018 IEEE Intelligent Vehicles Symposium (IV)*. IEEE, 2018.

[31] Woo, Hanwool, et al. "Lane-change detection based on vehicle-trajectory prediction." *IEEE Robotics and Automation Letters* 2.2 (2017): 1109-1116.

[32] Xie, Guotao, et al. "Vehicle trajectory prediction by integrating physics-and maneuver-based approaches using interactive multiple models." *IEEE Transactions on Industrial Electronics* 65.7 (2017): 5999-6008.

[33] Jeon, Hyeongseok, Junwon Choi, and Dongsuk Kum. "SCALE-Net: Scalable Vehicle Trajectory Prediction Network under Random Number of Interacting Vehicles via Edge-enhanced Graph Convolutional Neural Network." *arXiv preprint* arXiv:2002.12609 (2020).

[34] Zhao, Tianyang, et al. "Multi-agent tensor fusion for contextual trajectory prediction." *Proceedings of the IEEE Conference on Computer Vision and Pattern Recognition*. 2019.

[35] Wang, Wenshuo, et al. "A learning-based approach for lane departure warning systems with a personalized driver model." *IEEE Transactions on Vehicular Technology* 67.10 (2018): 9145-9157.

[36] Bahram, Mohammad, et al. "A game-theoretic approach to replanning-aware interactive scene prediction and planning." *IEEE Transactions on Vehicular Technology* 65.6 (2015): 3981-3992.

[37] Schreier, Matthias, Volker Willert, and Jürgen Adamy. "An integrated approach to maneuver-based trajectory prediction and criticality assessment in arbitrary road environments." *IEEE Transactions on Intelligent Transportation Systems* 17.10 (2016): 2751-2766.

[38] Alahi, Alexandre, et al. "Social lstm: Human trajectory prediction in crowded spaces." *Proceedings of the IEEE conference on computer vision and pattern recognition*. 2016.

[39] Cheng, Hao, and Monika Sester. "Modeling mixed traffic in shared space using lstm with probability density mapping." *2018 21st International Conference on Intelligent Transportation Systems (ITSC)*. IEEE, 2018.

[40] Huang, Yingfan, et al. "STGAT: Modeling Spatial-Temporal Interactions for Human Trajectory Prediction." *Proceedings of the IEEE International Conference on Computer Vision*. 2019.

[41] Xin, Long, et al. "Intention-aware long horizon trajectory prediction of surrounding vehicles using dual lstm networks." *2018 21st International Conference on Intelligent Transportation Systems (ITSC)*. IEEE, 2018.

[42] Min, Kyushik, et al. "RNN-Based Path Prediction of Obstacle Vehicles With Deep Ensemble." *IEEE Transactions on Vehicular Technology* 68.10 (2019): 10252-10256.
[43] Xing, Yang, Chen Lv, and Dongpu Cao. "Personalized Vehicle Trajectory Prediction Based on Joint Time Series Modeling for Connected Vehicles." *IEEE Transactions on Vehicular Technology* (2019).
[44] Hou, Lian, et al. "Interactive trajectory prediction of surrounding road users for autonomous driving using structural-LSTM network." *IEEE Transactions on Intelligent Transportation Systems* (2019).
[45] Kuefler, Alex, et al. "Imitating driver behavior with generative adversarial networks." *2017 IEEE Intelligent Vehicles Symposium (IV).* IEEE, 2017.
[46] Kosaraju, Vineet, et al. "Social-bigat: Multimodal trajectory forecasting using bicycle-gan and graph attention networks." *Advances in Neural Information Processing Systems.* 2019.
[47] Punzo, Vincenzo, Maria Teresa Borzacchiello, and Biagio Ciuffo. "On the assessment of vehicle trajectory data accuracy and application to the Next Generation SIMulation (NGSIM) program data." *Transportation Research Part C: Emerging Technologies* 19.6 (2011): 1243-1262.
[48] Coifman, Benjamin, and Lizhe Li. "A critical evaluation of the Next Generation Simulation (NGSIM) vehicle trajectory dataset." *Transportation Research Part B: Methodological* 105 (2017): 362-377.
[49] Foiadelli, Federica, Michela Longo, and Seyedmahdi Miraftabzadeh. "Energy consumption prediction of electric vehicles based on big data approach." *2018 IEEE International Conference on Environment and Electrical Engineering and 2018 IEEE Industrial and Commercial Power Systems Europe* (EEEIC/I&CPS Europe). IEEE, 2018.
[50] Xing, Yang, et al. "Energy oriented driving behavior analysis and personalized prediction of vehicle states with joint time series modeling." *Applied Energy* 261 (2020): 114471.
[51] Speidel, Oliver, et al. "Towards Courteous Behavior and Trajectory Planning for Automated Driving." *2019 IEEE Intelligent Transportation Systems Conference (ITSC).* IEEE, 2019.
[52] Shafiq, Muhammad, et al. "Data Mining and Machine Learning Methods for Sustainable Smart Cities Traffic Classification: A Survey." *Sustainable Cities and Society* (2020): 102177.

Yang Xing received his Ph. D. degree from Cranfield University, UK, in 2018. He is currently a Research Fellow with the Department of Mechanical and Aerospace Engineering at Nanyang Technological University, Singapore. His research interests include machine learning, driver behavior modeling, intelligent multi-agent collaboration, and intelligent/autonomous vehicles. His work focuses on the understanding of driver behaviors using machine-learning methods, and intelligent and automated vehicle design. He received the IV2018 Best Workshop/Special Issue Paper Award. Dr. Xing serves as a Guest Editor for IEEE Internet of Thing, IEEE Intelligent Transportation Systems Magazine, and Frontiers in Mechanical Engineering. He is an active reviewer for IEEE Transactions on Intelligent Transportation Systems, Vehicular Technology, Industrial Electronics, and IEEE/ASME Transactions on Mechatronics, etc.

Chen Lv is currently an assistant professor at Nanyang Technology University, Singapore. He received a Ph.D. degree at the Department of Automotive Engineering, Tsinghua University, China in 2016. From 2014 to 2015, he was a joint Ph.D. researcher at EECS Dept., University of California, Berkeley. His research focuses on cyber-physical systems, hybrid systems, advanced vehicle control, and intelligence, where he has contributed over 40 papers and obtained 11 granted China patents. Dr. Lv serves as a Guest Editor for IEEE/ASME Transactions on Mechatronics, IEEE Transactions on Industrial Informatics and International Journal of Powertrains, and an Associate Editor for International Journal of Electric and Hybrid Vehicles, International Journal of Vehicle Systems Modelling and Testing, International Journal of Science and Engineering for Smart Vehicles, and Journal of Advances in Vehicle Engineering. He received the Highly Commended Paper Award of IMechE UK in 2012, the National Fellowship for Doctoral Student in 2013, the NSK Outstanding Mechanical Engineering Paper Award in 2014, the Tsinghua University Graduate Student Academic Rising Star Nomination Award in 2015, the China SAE Outstanding Paper Award in 2015, the 1st Class Award of China Automotive Industry Scientific and Technological Invention in 2015, and the Tsinghua University Outstanding Doctoral Thesis Award in 2016.

Xiaoyu Mo received the B.E. degree from Yangzhou University, Yangzhou, China, in 2015, the M.E. degree from Huazhong University of Science and Technology, Wuhan, China, in 2017. He was a research associate with Nanyang Technological University, Singapore, from Sep. 2017 to Jan. 2019. He is now a Ph.D. student at Nanyang Technological University. His research interests include trajectory prediction and decision making for connected autonomous vehicles.

Chao Huang was born in China in 1990. She received the B.Sc. degree in automation from China University of Petroleum, Beijing, China, in June 2012, and the Ph.D. degree from the University of Wollongong, Wollongong, NSW, Australia, in 2018. She is currently a Research Fellow with the School of Mechanical and Aerospace Engineering, Nanyang Technological University. Her current research interests include human-machine shared control system, path planning for autonomous vehicle.

Zhongxu Hu received a mechatronic Ph.D. degree in 2018 from the Huazhong University of Science & Technology of China. He was a senior engineer at Huawei. He is currently a Research Fellow within the AUTOMAN group of Nanyang Technological University in Singapore. His current research interests include computer vision and machine learning applied to driver behavior analysis, autonomous vehicle in multiple scenarios.

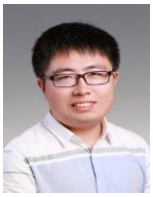

Peng Hang received the Ph.D. degree with the School of Automotive Studies, Tongji University, Shanghai, China, in 2019. He has been a Visiting Researcher with the Department of Electrical and Computer Engineering, National University of Singapore, Singapore, in 2018. Now, He is a Research Fellow with the Department of Mechanical and Aerospace Engineering, Nanyang Technological University, Singapore. His research interests include vehicle dynamics and control for driver-assistance systems, decision making, motion planning and motion control of autonomous vehicles.